AUTHIGENIC KAOLINITE AND MICA
AS EVIDENCE FOR PHASE EQUILIBRIA
AT LOW TEMPERATURES

by

R. W. REX*

California Research Corporation, La Habra, California

ABSTRACT

ELECTRON micrograph, X-ray diffraction, and chemical studies of secondary clay minerals formed within sandstones provide data supporting a portion of the phase relationships proposed by Garrels (Garrels and Christ, 1965) for kaolinite and K-mica growing in equilibrium with K-feldspar and quartz at about 25°C. A true phase distinction between mica and kaolinite is found at the phase boundary and not a continuous solid–solution series, such as proposed by Keeling (1961). Some of the micas, however, show evidence for the presence of an interlayer impurity, such as small amounts of hydroxymagnesium cation proxying for K^+. Electron micrographs and diffraction studies show epitaxial growth of oriented mica crystals on kaolinite providing evidence for the existence of these two distinct phases in mutual equilibrium with the solution from which they crystallized.

INTRODUCTION

EQUILIBRIUM phase relationships between mica, kaolinite, and K-feldspar at 25°C are difficult to determine. The reasons for this difficulty are numerous. Reactions in natural systems are often very slow, and are difficult to reproduce at low temperatures under laboratory conditions. Mineral dissolution at room temperature by hydrolysis offers one technique for estimating the position of phase boundaries. Extrapolation of high temperature data to low temperatures also provides a method for estimating low temperature thermodynamic equilibria.

Garrels (Garrels and Christ, 1965) (Fig. 1) has described his best estimates of equilibrium in the system $K_2O–Al_2O_3–SiO_2–H_2O$ in terms of the ratio of the log of the H_4SiO_4 concentration to the log of the potassium : hydrogen–ion ratio in solution. These phase diagrams were compiled by Garrels from the relationships given in Table 1, which are the best estimates currently available and are subject to further refinement.
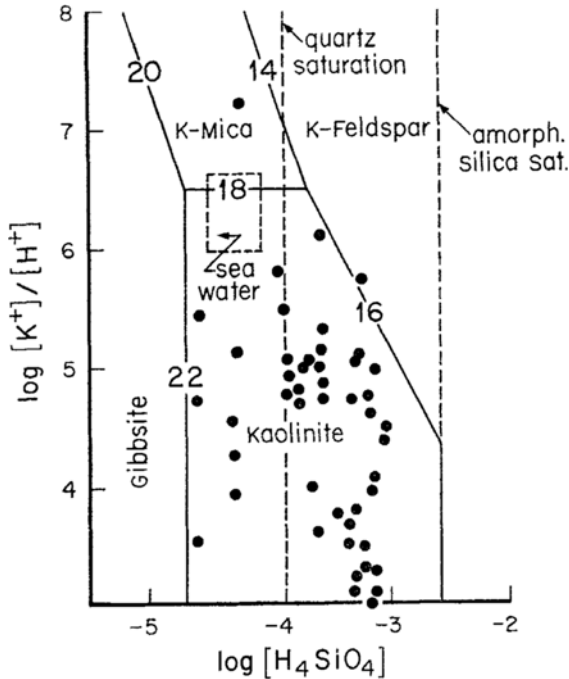
* Box 446, La Habra, California.

95

FIG. 1. Stability relations of some phases in the system $K_2O–Al_2O_3–SiO_2–H_2O$ at 25°C and 1 atmosphere, as functions of $[K^+]/[H_4SiO_4]$. Numbers in boundary lines refer to equations. Solid circles represent analyses of waters in arkosic sediments.

It is often useful to look for natural materials that occur along various phase boundaries in this type of system to try to gain some clue as to the validity of the diagram. I have been studying the area immediately adjacent to the join : kaolinite, K-mica and K-feldspar, trying to determine the nature of the mineral phases in equilibrium with each other. Keeling (1961) proposed that a continuous solid–solution series exists between mica and kaolinite. Our electron micrograph, electron diffraction, X-ray diffraction, and chemical analyses of secondary clay minerals crystallized within sandstones indicate that discrete phase boundaries occur between kaolinite, K-mica, and K-feldspar in agreement with the suggestions of Yoder and Eugster (1955, p. 272).

This study has been based primarily on clay fractions extracted from quarry samples of the Berea sandstone, Berea, Ohio; Entrada sandstone, Grand Junction, Colorado; St. Peter sandstone, Klondike, Missouri; and the Roubidoux sandstone, Rolla, Missouri, although more than a score of additional sandstones were surveyed and gave similar analytical results. The abundant morphologically perfect crystals of kaolinite and mica found in
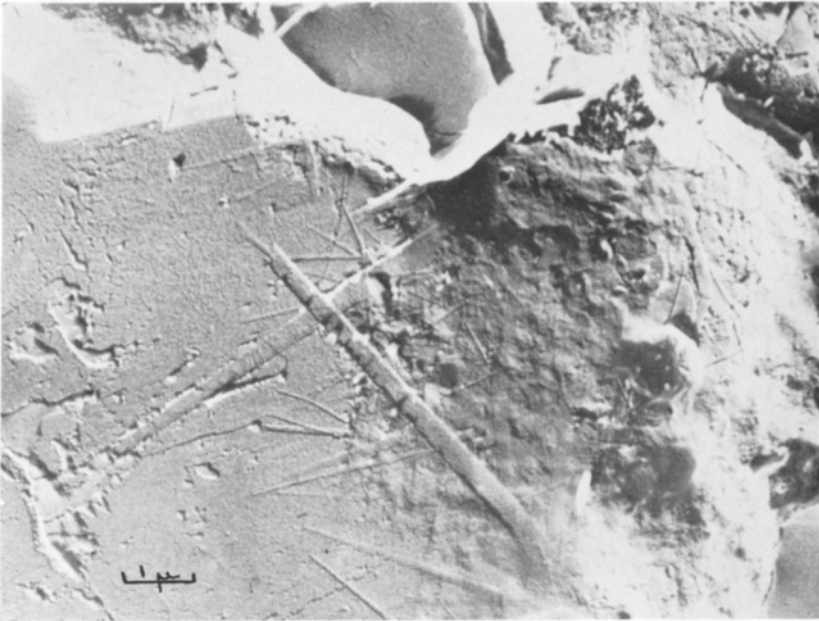
PLATE 1. Electron micrograph of a replica of a quartz sand grain from the Roubidoux sandstone showing numerous mica needles lying on the quartz surface. Polystyrene peel shadowed with chromium at 10 : 1 shadow angle.
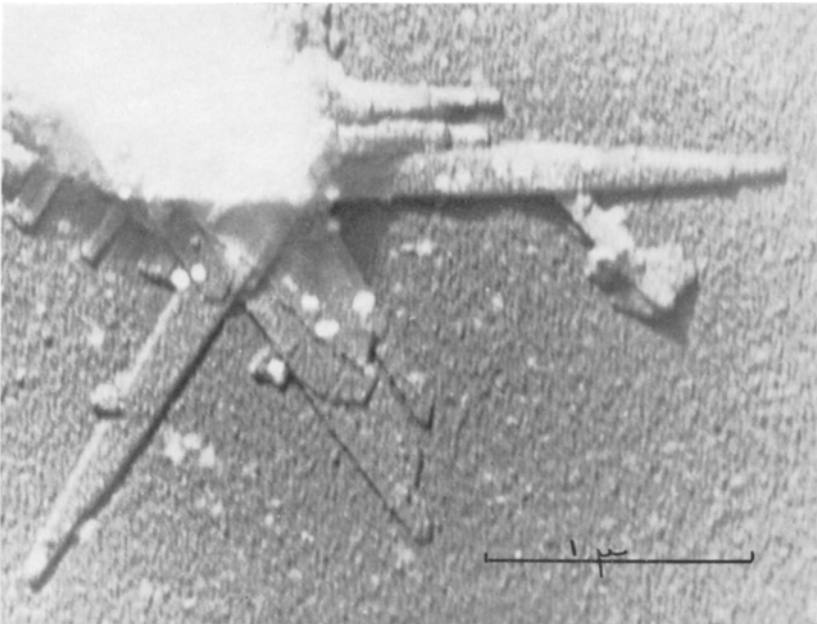

PLATE 2. Electron micrograph of a mica triplet twin lying on (001) and showing both (010) and (110) faces Clay from the Berea sandstone, shadowed with chromium at 10 : 1 shadow angle.
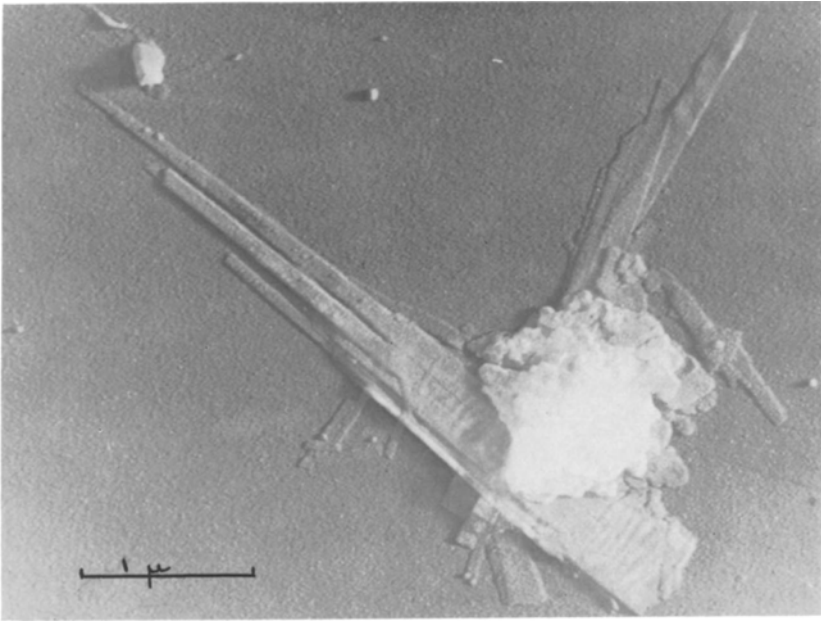
PLATE 3. Electron micrograph of mica needles and a cluster of small hexagonal kaolinite crystals from the Mirador sandstone, Colombia. Moiré fringes well-developed on multiple blades of mica crystals. Note delicacy of the smaller mica crystals. Shadowed with chromium at 10 : 1 shadow angle.
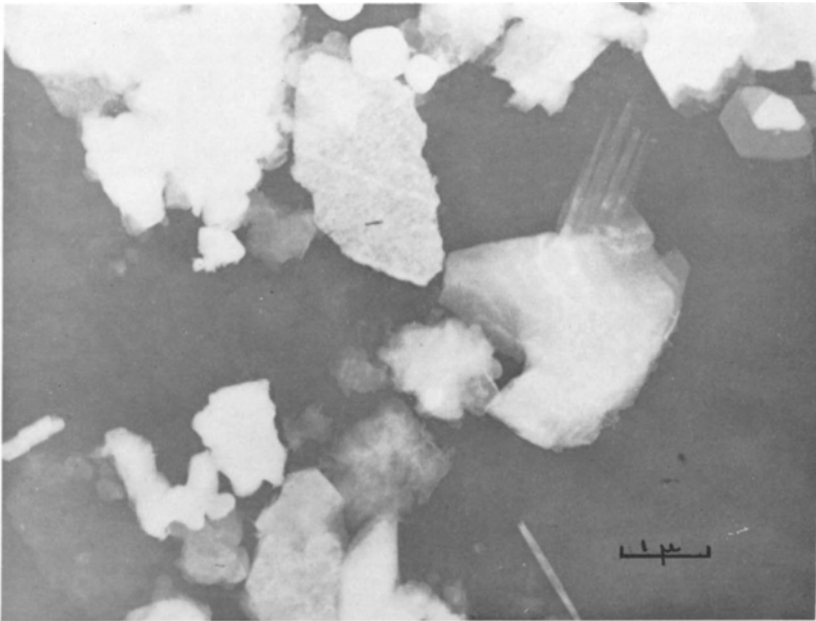

PLATE 4 Electron micrograph of a hexagonal kaolinite crystal with mica needles growing out from kaolinite, from the Berea sandstone. Not shadowed.
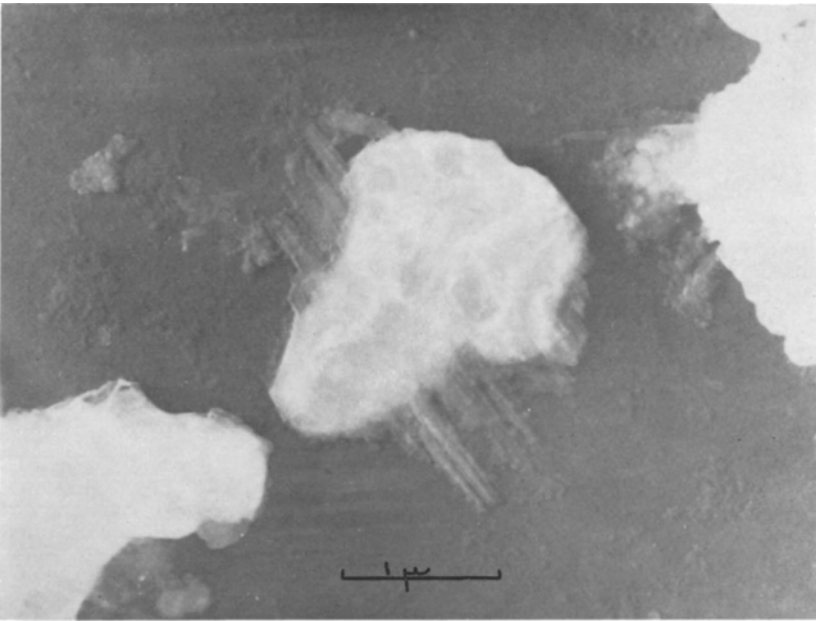
PLATE 5. Electron micrograph of a partially hexagonal kaolinite crystal with numerous mica needles extending beyond the perimeter of the kaolinite crystal. *x* and *y* of both phases appear to be parallel. Shadowed with chromium at 10 : 1 shadow angle. Berea sandstone.
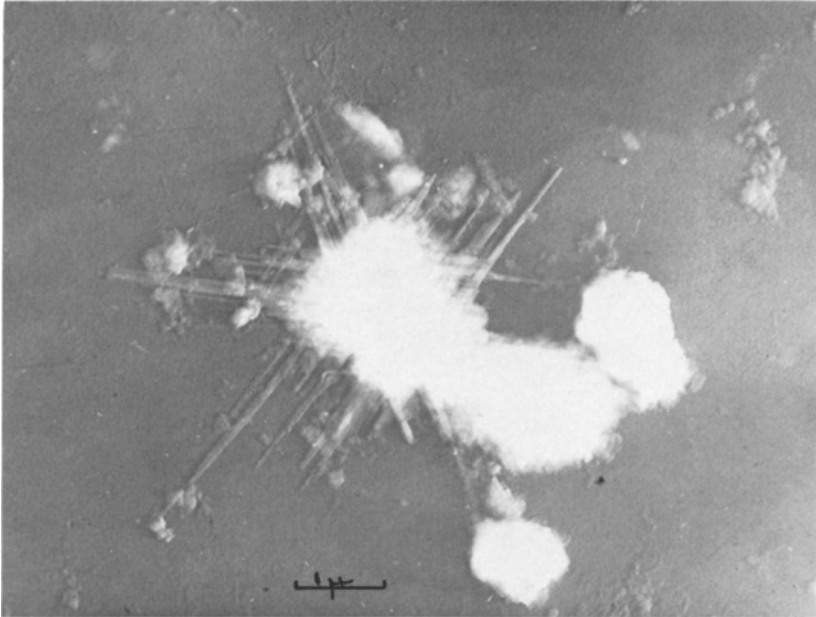

PLATE 6 Electron micrograph of a complex sixfold star of numerous delicate mica needles from the Roubidoux sandstone. Thick fluffy cluster, probably kaolinite, obscures core of mica star. Twinning of mica extensive on (001) composition plane. This photograph shows relatively rare secondary twins of needles growing on the tips of other needles. Shadowed with chromium at 10 : 1 shadow angle.
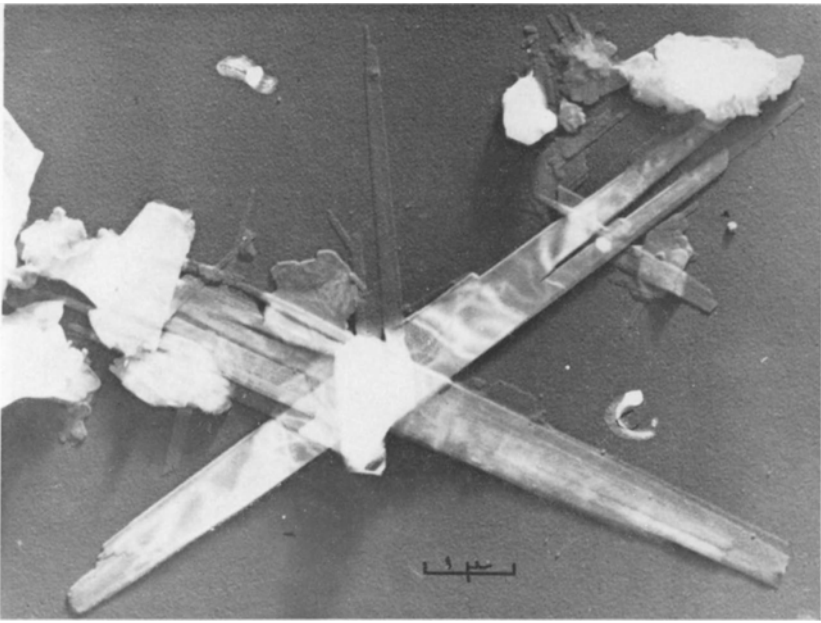
PLATE 7. Electron micrograph of mica needle star from the Mirador sand-stone, Colombia, showing a possible hexagonal kaolinite crystal at the core of the star. Note the drape of the single vertical mica crystal where it changes from its level in the (001) crystal plane to that of the substrate film. This shows that different blades of the star are in different planes of the (001). Note also the tendency of single blades to feather into multiple needles. Shadowed with chromium at 10 : 1 shadow angle.
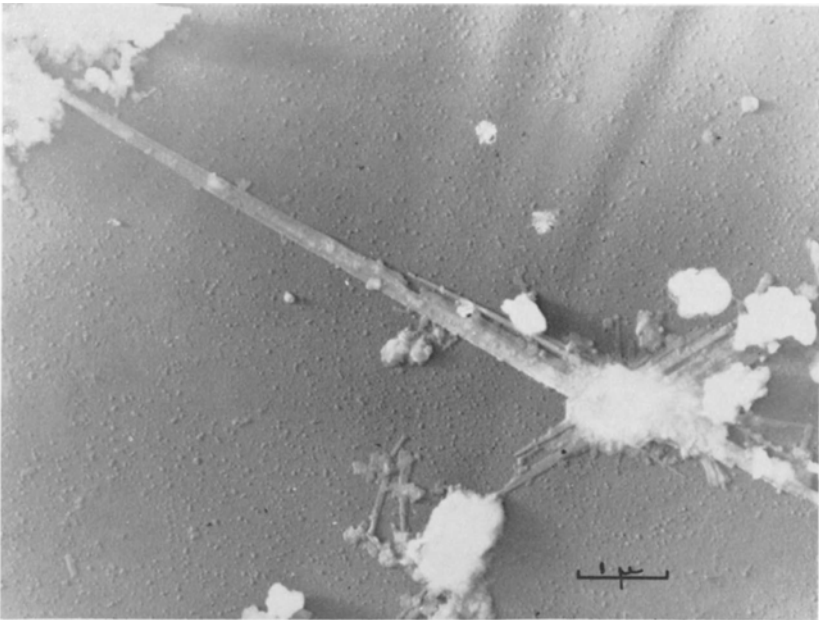
PLATE 8. Electron micrograph of a mica needle star, from the Roubidoux sandstone, showing a well-defined hexagonal kaolinite crystal at the core of the star. The original electron micrograph clearly shows hexagonal growth steps on the kaolinite crystal. Note the delicacy of the 6 μ-long mica needles, where the electron beam clearly shows small kaolinite crystals underneath the mica. Shadow length measurements of the smallest needles suggest a thickness of 20–40 Å. Shadowed with chromium at 10 : 1 shadow angle.

Table 1.—Equations Used by Garrels in Preparing the Phase Diagram in Fig. 1.

Equations	
14:	K-mica/K-feldspar join
	$\log K_1 = -4.9 = \log \dfrac{[K^+]}{[H^+]} + 3 \log [H_4SiO_4]$
16:	K-feldspar/Kaolinite join
	$\log K_2 = -1.0 = \log \dfrac{[K^+]}{[H^+]} + 2 \log [H_4SiO_4]$
18:	K-mica/Kaolinite join
	$\log K_3 = +6.5 = \log \dfrac{[K^+]}{[H^+]}$
20:	Gibbsite/K-mica join
	$\log K_4 = -7.6 = \log \dfrac{[K^+]}{[H^+]} + 3 \log [H_4SiO_4]$
22:	Gibbsite/Kaolinite join
	$\log K_4 = -4.7 = [H_4SiO_4]$

these sands have been the objects of this study. The use of quarry materials suggests that the sandstones studied have been subjected to water salinities fresher than sea water for a long time and that therefore our data do not necessarily apply to sea water in which sodium concentrations are higher.

MINERALOGY

K-Mica–Kaolinite–K-Feldspar

Careful fractionation of the clays from the sandstones on the basis of size followed by electron microscopy, electron diffraction, X-ray diffraction and chemical analysis shows pseudohexagonal crystals of kaolinite and long, very thin needle-shaped crystals of dioctahedral potassium mica (Plates 1 to 8). The kaolinite crystals are of varying size, ranging from a few tens of millimicrons to 4 or 5 μ in diameter. They often grow in clusters, although single crystals are common. The mica needles occur in a variety of habits. They range from 0.1–5 μ in length, 0.01–0.1 μ in width and are usually less than 0.01 μ thick. The thinness of many of the mica crystals is startling. The bright field electron micrographs shown in this paper were shadowed with chromium metal to give a shadow ten times as long as the object is high. The shadows of many of the needles range from 100–600 Å wide (Plates 2 and 3). Consequently, the individual crystals should be from 10–60 Å thick or one to six unit cells thick. It is hard to believe that these thin needles of mica are strong enough to survive handling, and the problem is being studied further.

Occasional mica crystals are doubly terminated needles. A few show (110) faces as well as the (010), and all show well developed (001) faces (Plate 2). The mica–needle crystals commonly occur in closely parallel clusters and moiré fringes are commonly observed (Plate 3). In some cases mica crystals grow out of single kaolinite crystals (Plates 4 and 5). In other cases twinned

mica crystals occur with three sets of needles having (001) composition planes with rotation of 180° around [310] as a twin axis or by rotation 120° around [001] (Plates 2, 6 and 7). These twins usually have a large crystal at the core of the twin that is hard to identify (Plates 6 and 7). In a few cases it is possible to observe that a pseudohexagonal kaolinite crystal constitutes the core of the mica twin (Plate 8). These six-pointed star-shaped twins are common in the 0.5–2 μ fraction of the St. Peter sand and fairly common in the Roubidoux sandstone. They are scarce but also present in the Entrada and Berea sandstones.

Electron diffraction studies of single mica needles show that they are elongated parallel to x, lie on (001), and their (020) spacings correspond most closely to that of dioctahedral K-mica or illite (4.50 Å) (Plate 9). X-ray diffraction studies give an (001) spacing of 10.0–10.4 Å. Bright field electron microscope inspection suggests that most of the mica star twins growing on kaolinite have their y-axes parallel or rotated 60°, or some multiple thereof, with respect to the y-axis of their core kaolinite crystal, as defined by its expected morphology of (010), (110), and (001). However, electron diffraction studies of a St. Peter specimen showed a 30° rotation of the kaolinite y-axis from that of the three twinned mica crystals (Plates 10, 11 and 12). In any case, these electron diffraction photographs prove that the mica and kaolinite
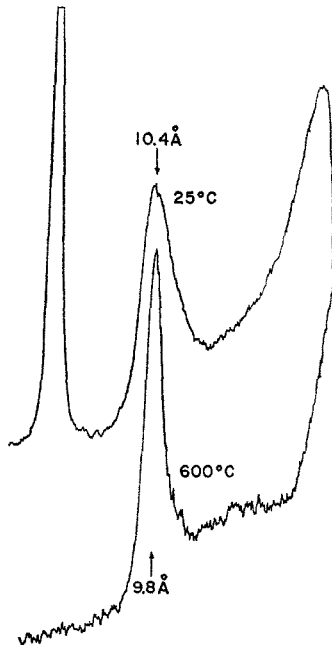

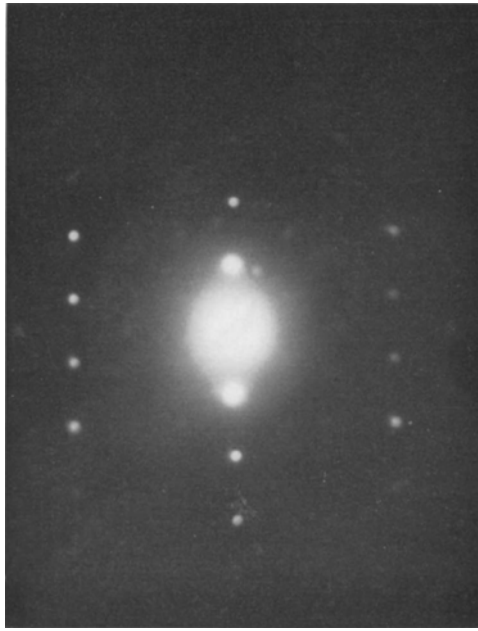Fig. 2. Clay fraction of the St. Peter Sandstone, Klondike, Mo.

PLATE 9. Selected area electron diffraction pattern of a single mica needle from the St. Peter sandstone. The two brightest inner spots are (020), and parallel to these are the first layer lines. Defocused images show that the needles are elongated parallel to their x-axes. All mica crystals lie on (001).

PLATE 10. Selected area electron diffraction pattern of a sixfold mica star growing symmetrically on a kaolinite crystal core from the St. Peter sandstone. The six brightest inner spots are the three pairs of (020) spots contributed by the three mica needles. There is a single pair of weak spots at the same radius corresponding to the (020) of the kaolinite, rotated 30° from those of the mica (020). For a defocused image of same cluster see Plate 11. Note evidence that all grains are lying on their (001) as there are no inner spots larger than the 4.50 Å of the (020).
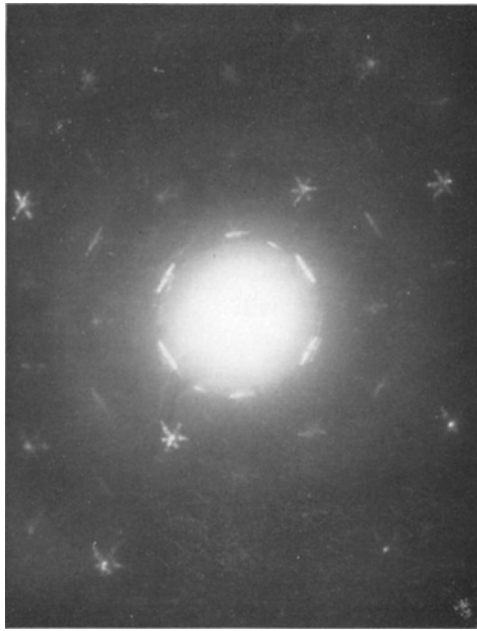
PLATE 11. Selected area electron diffraction pattern of the same sixfold mica star shown in Plate 10. Defocusing shows the six images of the three single mica crystals that contribute the six bright (020) mica spots in Plate 10. Likewise the (020) image of the kaolinite remains as spots because of the small hexagonal character of the core crystal. Other spots in pattern can all be assigned to individual mica crystals or to the entire sixfold star twin. Mica crystal elongation parallel to the x-axis illustrated by (020) images Plates 10 and 11 demonstrate criteria for epitaxial orientation of mica on kaolinite
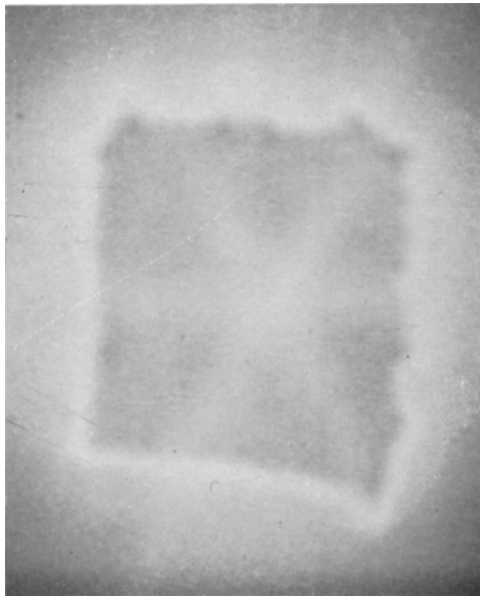

PLATE 12. Bright field image of the star shown in Plates 10 and 11 enlarged from the center of Plate 11. Jamming of the electron microscope plate carrier prevented normal bright field micrograph being obtained to accompany the diffraction photographs.

crystals have their structures mutually systematically oriented and therefore growing in epitaxial relationship.

The X-ray data suggest that the mica crystals, although morphologically perfect, do not have the ideal muscovite structure. We find the (001) is usually 10.1–10.4 Å. The (001) line changes shape somewhat on heat treatment (Figs. 2, 3) with peak sharpening and intensity loss observed on heating of the St. Peter, Roubidoux and Entrada from 110°C to 650°C suggesting that we are driving off water. The Berea mica showed no peak shift on heating, suggesting that it has a composition closer to ideal muscovite than the micas from the other three sandstones (Fig. 4). Solid solution of various cations is common in micas (Yoder and Eugster, 1955) and probably causes the observed anomalous (001) spacing. The dehydration, chemical and X-ray data on the authigenic micas suggest the presence of a small amount of impurity material proxying for K^+ in the interlayer position. My data are insufficient to identify the impurity definitively but are suggestive of traces of magnesium hydroxide in the interlayer position. Several causes of the excessive (001) spacing were considered, including isomorphous substitution of Na^+, OH_3^+, and NH_4^+ for the K^+. The low Na^+/K^+ shown in Table 2, and very low NH_4^+ (N_2 analyzed by micro-Dumas method) argued against the importance of Na^+ and NH_4^+. Several lines of evidence make OH_3^+ improbable, although not proved to be absent. The thermal dehydration of the mica by heating to 550°C. causes a nearly 50 per cent loss in (001) peak intensity
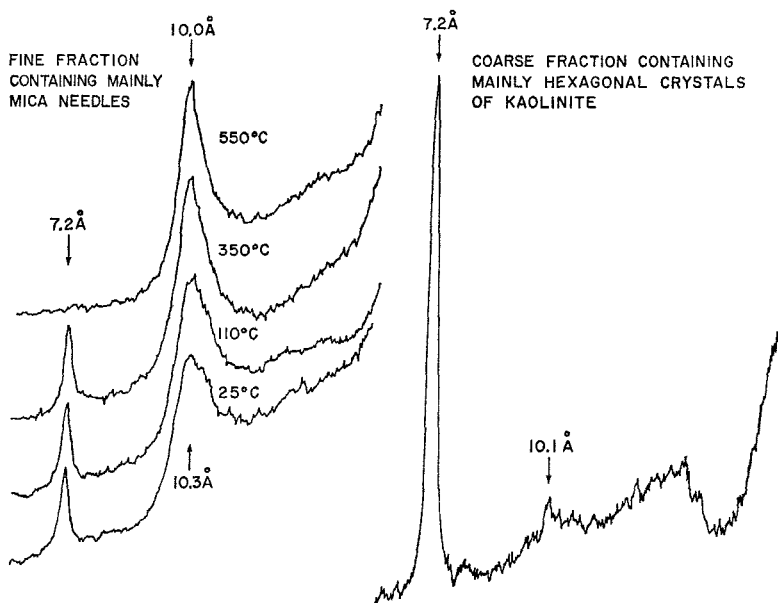

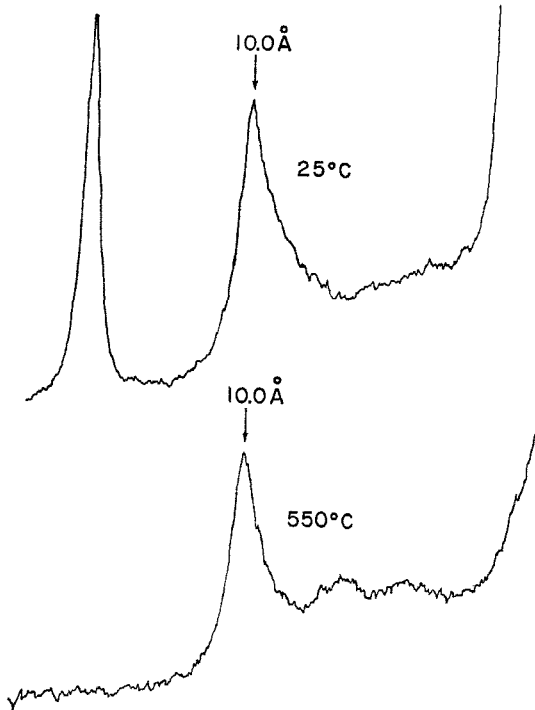FIG. 3. Clays extracted from the Roubidoux Sandstone, Rolla, Mo.

FIG. 4. Clay fraction of Berea Sandstone, Berea, Ohio.

Hydrobiotite, vermiculite, montmorillonite etc. all show (001) intensity increases at 10 Å as a consequence of dehydration. Furthermore, there is considerable doubt that oxonium micas can exist in thermodynamic equilibrium with natural pore–water solutions of pH 6–8, expected for the formation of the authigenic micas described here. Schwertmann and Jackson (1964) have shown that under natural conditions aluminous oxonium clays liberate aluminum from their structure. This aluminum reacts with the ion exchangeable oxonium to produce interlayer hydroxyaluminum polymers. This instability of oxonium clay minerals therefore makes it unreasonable to propose oxonium as the impurity responsible for the 10.1–10.4 Å (001) spacings of some of the authigenic micas. Another possible explanation for the anomalous spacing is the presence of small amounts of interlayer hydroxyaluminum polymer, such as that described by Jackson (1963) for many soil clays. This implies a slight excess of aluminum in the pore solution at the time of mica–crystal growth. The pore–water chemical system is in equilibrium with an effectively infinite reservoir of silica in a sandstone, making it unlikely that hydroxyaluminum should survive in solution in sufficient

TABLE 2.—COMPARISON OF THE CHEMICAL COMPOSITION OF CLAY FRACTIONS STUDIED
WITH OTHER CLAY MINERALS.

	Clay Fractions[1]	Kaolinite[2]	Muscovite[3]	Illite[4]
K_2O/Na_2O	16–47	?	17	12
K_2O/Al_2O_3	0.21–0.26	0.001	0.26	0.28
Al_2O_3/MgO	9–12	280	380	9
SiO_2/Al_2O_3	1.6–3.1	1.2	1.2	3.2

[1] This study.   [2] Nagasawa, 1953.   [3] Hurlbut, 1956.   [4] Kerr and Pill, 1950.

concentration to appear in the structure of the micas. The silica : alumina data in Table 2 support this argument showing silica : alumina values anomalously large for muscovite. Therefore, hydroxyaluminum polymers are probably not the cause of the anomalous (001) spacing. An alternate hypothesis suggested by M. L. Jackson (personal communication) is the presence of hydroxymagnesium polymeric cations in analogous structural relation to the hydroxyaluminum polymeric cations. The common isostructural relationships of magnesium and aluminum hydroxides are well-known. The chemical data indicate excessive amounts of magnesium for muscovite or kaolinite. The X-ray data (Fig. 3) show the presence of small amounts of 14 Å material in some samples suggesting the possibility of chlorite-type mixed layering appearing as a consequence of the substitution of hydroxymagnesium for K^+ in the interlayer space. I have obtained two selected area electron diffraction photographs of microtome slices of mica needles that yielded 14 Å spacings. The contributing crystals must have been exceedingly thin, since it has usually been impossible for me to obtain (001) electron diffraction images from microtome slices of 1 μ thickness. This suggests the possibility of a small amount of very delicate chlorite probably also of authigenic origin.

My data support the hypothesis that hydroxymagnesium polymeric cations proxy for K^+ on the mica interlayer surface causing slight distortion of the (001) surface. The bulk of the hydroxymagnesium cation would help explain a number of other observed phenomena. It is possible that the atomic scale irregularity caused by the presence of a hydroxymagnesium cation could cause the tilt between successive (001) layers that produces the commonly observed moiré fringes (Plate 3). The local discontinuity of a hydroxymagnesium cation might also block mica growth in the (001) plane along the observed elongation direction of the x-axis. This could be the mechanism for splitting a single mica sheet into multiple needles (Plates 1–8).

Spectrographic analysis of separated clay fractions (Table 2) shows that $K_2O : Na_2O$ ratios are comparable to muscovite, $Al_2O_3 : MgO$ are low and comparable to illite but not kaolinite or muscovite, $SiO_2 : Al_2O_3$ are high and closest to illite and $K_2O : Al_2O_3$ comparable to both muscovite and illite. These clay fractions showed no quartz or feldspar diffraction peaks (Fig. 5). We interpret these data combined with the (001) : (002) : (003) intensity data
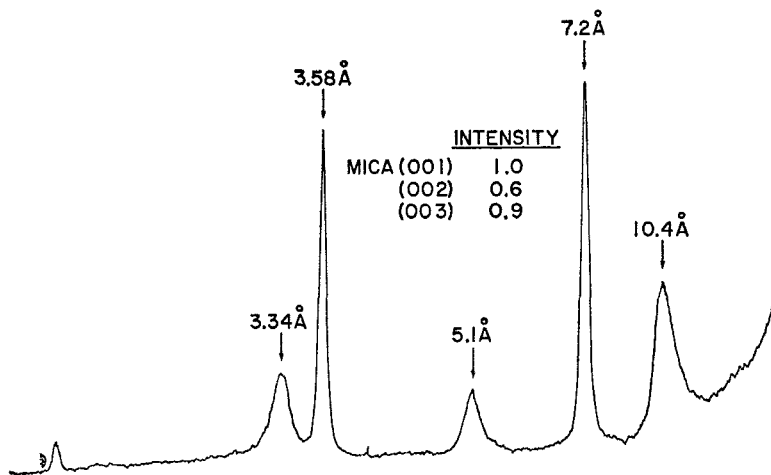
FIG. 5. Clays extracted from the St. Peter Sandstone, Klondike, Mo.

(Fig. 5) and the b-parameter to indicate that the micas in the clays are potassium dioctahedral micas containing more silica and magnesium and less potassium than normal for muscovite. A number of properties all point to the similarity between these delicate but morphologically perfect mica crystals and illite. The thinness of our mica crystals gives rise to (001) X-ray diffraction line broadening; the y-axis unit–cell dimension of 9.00 Å corresponds to the value accepted by Deer, Howie, and Zussman (1962, p. 213); and the silica and magnesium excess and potassium deficiency all agree with illite. Velde (1965) has proposed that illite is actually a K-mica with a small measure of mixed layering with chlorite. He also shows data for hydrothermal syntheses at several hundred degrees temperature supporting the existence of an equilibrium mica–chlorite mixed-layer assemblage. My data on natural low temperature micas supports Velde's proposal that this type of mixed layering occurs at low temperatures.

The details of the crystallography of the epitaxial mica twins on kaolinite will be treated in a paper to be published elsewhere. The important point relevant to the phase relationships is that exceedingly delicate and morphologically perfect crystals of K-mica and kaolinite should be in chemical equilibrium with each other where they grow in this epitaxial relationship. Therefore, the compositions of the cojoining pair define a portion of their mutual phase boundary.

GEOLOGICAL APPLICATIONS

Our data suggest that weathering of K-feldspar in sandstones, such as those studied, results in two stages of kaolinite growth. Large crystals of kaolinite form initially, many of them with mica–crystal overgrowths, some

of them in epitaxial relationship. No large kaolinite crystals have been found growing out from mica crystals, suggesting that the large kaolinite crystals formed first. In addition to the large kaolinite crystals, we find additional numerous, small, often morphologically perfect, kaolinite crystals and numerous small mica needles often coating the larger crystals. This suggests that kaolinite crystallizes initially and then is followed by the simultaneous growth of both kaolinite and mica. We interpret these data to mean that we are initially growing kaolinite in its stability field along the K-feldspar join by dissolution of K-feldspar. As the concentration of K^+ increases as a consequence of K-feldspar dissolution, the fluid composition changes in a direction towards the mica–kaolinite join. Mica and kaolinite then form together as a consequence of the solution of K-feldspar as long as it is present. This three-phase join appears to be a point of geochemical convergence for weathering of diverse lithologies of sandstone. K-feldspar is observed to be selectively destroyed in sandstones and we therefore assume that it is the most soluble component. Experimental data on the low temperature solubility of K-feldspar would be most helpful but are not known to be available now.

CONCLUSIONS

There is considerable evidence for a phase join between K-feldspar, K-mica and kaolinite where the pore water has low salinity. It is also possible that a minor degree of mixed layering occurs in the K-mica phase as a consequence of the substitution of hydroxymagnesium cations for K^+ in the interlayer position. These data support the proposed phase relationships suggested by Garrels (Garrels and Christ, 1965) for a portion of the system K-mica–kaolinite–K-feldspar. The proposal of Keeling (1961) concerning the existence of solid solution between kaolinite and K-mica is inconsistent with this observation.

ACKNOWLEDGMENTS

REFERENCES

Deer, W. A., Howie, R. A., and Zussman, F. (1962) *Rock-Forming Minerals*, vol. 3, *Sheet Silicates*, p. 213, Longmans, London.
Garrels, R. (1965) *Solutions, Minerals and Equilibria* (Edited by R. Garrels and C. L. Christ), ch. 10, Harper & Row, New York.

8

HURLBUT, C. S., JR. (1956) Muscovite from Methuen Township, Ontario, *Am. Mineralogist* **41**, 892.

JACKSON, M. L. (1963) Aluminum bonding in soils. A unifying principle in soil science, *Soil Sci. Soc. Am. Proc.* **29**, 1–10.

KEELING, P. S. (1961) A new concept of clay minerals, *Trans. Brit. Ceram. Soc.* **60**, 449–74.

KERR, P. F., and PILL, R. J. (1951) Analytical data on reference clay materials, *Reference Clay Minerals, American Petroleum Institute Research Project* 49, *Preliminary Report* 7, pp. 1–38, Columbia University, New York.

NAGASAWA, K. (1953) Kaolinite from the Mikana mine, Niigata prefecture, *J. Earth Sci., Nagoya Univ.* **1**, 9.

SCHWERTMANN, U., and JACKSON, M. L. (1964) Influence of hydroxy-aluminum ions on pH titration curves of hydronium aluminum clays, *Soil Sci. Soc. Am. Proc.* **28**, 179–83.

VELDE, B. This volume, pp. 29–32

YODER, H. S., and EUGSTER, H. P. (1955) Synthetic and natural muscovites, *Geochim. Cosmoschim. Acta* **8**, 225–80.